Robust flutter analysis using interval modal analysis and continuation method

Conference Paper · January 2009

Source: DLR

CITATION
1

READS
56

1 author:

Jan Schwochow
German Aerospace Center (DLR)
48 PUBLICATIONS **11** CITATIONS

SEE PROFILE

ROBUST FLUTTER ANALYSIS USING INTERVAL MODAL ANALYSIS AND CONTINUATION METHOD

J. Schwochow

Deutsches Zentrum für Luft- und Raumfahrt e.V., Institute of Aeroelasticity,
Bunsenstr. 10, 37073 Göttingen
e-mail: jan.schwochow@dlr.de

Keywords: Robust flutter analysis, interval modal analysis, interval flutter analysis, uncertainty propagation, Monte-Carlo-simulation, continuation method.

Abstract. For robust analysis of the flutter stability, it is necessary to consider the uncertainties of the structural dynamics model. These uncertainties can be clarified from estimates of uncertainties of the parameters in finite element models or from statistical evaluations of experiments. As a supplement to the reliable flutter algorithm for solution of the flutter equation, the continuation method is introduced, which allows the specific examination of individual solution branches of the flutter equations that risk being critical for stability. To compute the range of variations of eigenfrequencies and mode shapes caused by possible structural uncertainties, the interval modal analysis is introduced. The interval modals are tracked through the flutter stability analysis. The deterministic computed intervals of critical flutter speeds are compared to the probabilistic results obtained by Monte-Carlo-simulation.

1 INTRODUCTION

Flutter is a self-excited vibration that can occur with elastic structures that are subject to airflow when the interaction of deflection and the induced air forces transmit energy from the flow into the oscillation of the structure. This may lead to damage or destruction of the vibrating structure. The examination of the dynamic stability of an aircraft requires the exact determination of the elastic behaviour, structural damping and inertia forces, as well as the aerodynamic forces in connection with the matched point flow parameters. For this purpose, suitable simulation models are set up that must be validated by experiments. Since simplifications are introduced in the theoretical formation of the models on one hand, and the measuring accuracy is limited in the experiment on the other, models and their parameters may include uncertainties, making it difficult to determine the dynamic stability boundaries. For the robust flutter analysis, it is necessary to propagate the effects of identified uncertainties towards aeroelastic stability of the aircraft to cover the uncertain-but-bounded parameter space. Robust stability is guaranteed when the uncertainties cannot destabilize the system. In recent years, the so-called μ-analysis from the control community has been applied to perform robust flutter analysis [11]. Borglund formulated the μ-k method [4], where the classical frequency-domain aeroelasticity of p-k and g methods ([10], [6]) are combined with μ-analysis. In this paper, a combined method is proposed which determines the lower and upper bounds of eigenfrequencies and mode shapes by the non-probabilistic interval modal analysis method from Sim and Qiu [16]. Then these bounds are tracked through the flutter stability analysis by applying the continuation method from Cardani and Mantegazza [5]. Each modal degree of freedom d.o.f. is continued for increasing flight velocity. After each continuation step, the bounds of aeroelastic damping and frequency are evaluated.

2 UNCERTAINTIES IN ROBUST FLUTTER ANALYSIS

For an efficient and reliable aeroelastic certification process, the uncertainties in the aerodynamic and structural dynamic modelling must be estimated in order to decide whether they can be tolerated or must be push under an uncritical threshold value. The analysis must look for the most unfavourable combination of the essential parameters (worst case) in order to ensure safe operation in the entire flight envelope.

The stability analysis assumes that the vibration of the airplane in free flight is composed of rigid body modes, vibration modes of the airframe and deflection of control surfaces through linear superposition. The eigenfrequencies and mode shapes can be determined during the developmental process through modal analysis based on the finite element method. It is generally necessary, however, before the first flight, to check the structural models of the airplane by conducting a ground vibration test on the first prototype. Possible deviations between the model and experiment reflect the structural dynamic uncertainties for the ensuing proof of stability. For small airplanes, structural dynamic models are usually not available, so that one must solely rely upon the measured modal data including measurement noise.

The numerical modelling of structural dynamics of the aircraft is based on simplifications of the actual structure and is conducted in connection with parameters that determine geometry, material characteristics and boundary conditions. The determining physical parameters include uncertainties, whose causes can be divided as follows:

Intentional simplifications: Individual dynamic effects are rendered simplified because the expenditure of possible refinement is disproportionate to the resulting improvement. For example, the dynamic modelling of the mechanical or hydraulic control system of an airplane is simplified to an equivalent system of spring and damping elements.

Dynamics that are unknown or cannot be modelled: This group comprises of dynamic features that influence the system behaviour, but are unknown. Friction or free-play in the airplane structure or in the control system can often not be represented in FE-models. Furthermore, the vibration modes are usually only determined on the unstressed airplane.

Parameter uncertainties: Even if the model renders physically correct the individual influences, quantitative inaccuracies can still result in parametric uncertainties. For example, the modulus of elasticity is dependent on the load path, especially in composite components.

Stochastic uncertainty factors: This group consists of uncertainties that overlap in reality and therefore can never be exactly determined. Due to production inaccuracies, the modulus of elasticity varies for bolt and rivet joints for example. The resin to fibre ratio influences the weight of the composite components. For experimental data, measurement noise generally shows stochastic nature.

To ensure flutter-free operation of the aircraft it is convenient to describe the identified structural uncertainties as perturbation parameters based on a nominal model. Different approaches can be applied to determine the deviation of the nominal model. The methods can be distinguished in probabilistic and non-probabilistic concepts. In Monte Carlo simulations [13] a random generator fills the vector of the uncertainty parameters, the system matrices are evaluated, and the modal analysis problem is solved. In order to obtain a statistically funded statement, many random combinations must be analyzed. Therefore, this procedure requires a high amount of computational work, but can be easily integrated into an existing process. In

the selection of the probability distribution for each entry, the state of knowledge of the variations of the parameters is reflected that is gained through experience or statistical evaluations. When determining the flutter stability for the certification of a new aircraft design, it must be assured that there is no danger of flutter for all combinations of the uncertain parameters up to the interval boundaries. For the non-probabilistic propagation of uncertain-but-bounded parameters in modal analysis, deterministic interval methods ([15], [16]) can calculate upper and lower bounds of natural frequencies and modal shapes in an efficient manner. For further decrease of the computational costs, transformation to adequate subspaces reduces the full order model in physical d.o.f to significantly lower orders. An expanded modal matrix approximates the vibration mode shapes of the modified structure using the nominal eigenvectors and their sensitivities with respect to the uncertain parameters or using families of eigenvectors calculated from the lower and upper bounds of the identified uncertain parameters.

In order to evaluate aeroelastic stability boundaries the established procedures for the solution of the flutter equations according to the p-k method [10] and the g-method [6] respectively must be expanded so that the dependencies of the stability towards upper and lower bounds of frequencies and modal shapes can be described. Although the flutter equations are formulated in modal d.o.f., the unsteady air loads depend upon the uncertainties in spatial distributions of modal deflections. In commercial aeroelastic codes, such as NASTRAN [18] or ZAERO [17], the stability analysis is conducted for the entire deterministic system with all d.o.f.. The modified system requires a completely new calculation. As an alternative in [5] and [14], the continuation method is suggested for the solution of the flutter equations. The non-linear system of flutter equations are solved in a direct manner for a free continued parameter. One single solution branch is tracked for increasing flight speed using a predictor-corrector procedure. For this purpose, the continuation method requires starting solutions, which are the modal results at zero flight speed. The advantage is seen in the specific stability examination of individual critical solution branches, which are active in the identified flutter mechanism without reduction or truncation of the entire system. In [12] the continuation method is used to analyse the effect of structural non-linearities in the flutter analysis dependent on the amplitude of control surface deflections.

3 DIRECT SOLUTION OF FLUTTER EQUATIONS

The flutter equations are generally set up in modal d.o.f. in the Laplace-domain:

$$\left([M_{hh}]s^2 + [C_{hh}]s + [K_{hh}] - \frac{1}{2}\rho_\infty V_\infty^2 \left[Q_{hh}(M_\infty, k) \right] \right) \{q\} = \{0\}, \qquad (1)$$

where $[M_{hh}] = [\Phi]^T [M][\Phi]$ is the generalized inertia matrix, $[C_{hh}] = [\Phi]^T [C][\Phi]$ is the generalized damping matrix, $[K_{hh}] = [\Phi]^T [K][\Phi]$ is the generalized stiffness matrix and $\left[Q_{hh}(M_\infty, k) \right]$ is the generalized aerodynamic loading matrix. The latter non-linearly depends on the Mach number M_∞ and the reduced frequency k, defined in the following way:

$$k = \frac{\omega c}{V_\infty} = \frac{\mathrm{Im}(s) c}{V_\infty}, \qquad (2)$$

where c is a specified reference length and V_∞ is the true undisturbed freestream velocity. The aerodynamic force matrix is pre-multiplied by the dynamic pressure, so that it depends quadratically on the freestream velocity and linearly on the air density. The calculation will

be further explained in Section 5. The eigenvector, $\{q\}$, of the generalized coordinates contains the complex participation factor of each mode shape. Depending on the sign of the real part, the eigenvalue s expresses a positively or negatively damped oscillation:

$$\{\overline{q}(t)\} = \mathrm{Re}\left[\{q\}\, e^{st}\right] = \mathrm{Re}\left[\{q\}\, e^{(\sigma+i\omega)t}\right]. \tag{3}$$

Since a description of the aerodynamic force matrix using the complex reduced frequency is not always available, the aerodynamic terms are usually required to be purely harmonic motion, even when the vibrations of the entire system increase or decrease. The assumption of aerodynamic forces caused by harmonic motion is justified for the weakly damped situation close to the flutter stability limit. It presents an approximation for more strongly damped solutions. The contents of the bracket in Eq. (1) can be interpreted as the aeroelastic coefficient matrix $[F]$ for the solution vector $\{q\}$:

$$\left[F\left(s, k, M_\infty, \rho_\infty\right)\right]\{q\} = \{0\}. \tag{4}$$

At flutter onset however, only one solution branch usually becomes unstable at the critical flutter speed. For examination of the uncertainty of this flutter velocity with regard to the uncertainties of the structural-dynamic model of the airplane, it makes sense to concentrate on this solution of the flutter equations and their variations. One should have a general overview of the flutter behavior by looking at the results of the established procedures. The p-k-method [10] and the g-method [6] iteratively solve the system of equations, whereby the starting value of the eigenvalue s and the flow velocity V_∞ are specified. Thereafter the critical solutions are pursued taking into account uncertainties defined in intervals. Reduction in the number of d.o.f. can often clarify the flutter mechanism.

Numerical continuation is a technique to generate successive points along a solution branch of a nonlinear equation system. Cardani and Mantegazza [5] developed an algorithm for the direct solution of the flutter equations using the continuation method to track various solutions dependent on free parameters. The solution vector $\{q\}$ of Eq.(4) is not determined in modulus and phase in the complex plane, which results in an infinite number of solutions. Only if one non-vanishing component is specified in modulus and phase, the system of equations has n-1 complex unknowns for $\{q\}$. The scaling together with an additional constraint for the relation of the imaginary part of the eigenvalue and the reduced frequency are introduced as additional equations

$$\{y\} = \begin{Bmatrix} \left[F\left(s, k, M_\infty, \rho_\infty\right)\right]\{q\} \\ \{q\}^T\{q\} - 1 \\ \mathrm{Im}(s) - \dfrac{V_\infty}{c} k \end{Bmatrix} = \{0\}. \tag{5}$$

The complex system of equations contains $2n+6$ unknowns

$$\{\hat{x}\}^T = \left\{\mathrm{Re}(q_1), \ldots, \mathrm{Re}(q_n), \mathrm{Im}(q_1), \ldots, \mathrm{Im}(q_n), \mathrm{Re}(s), \mathrm{Im}(s), k, V_\infty, M_\infty, \rho_\infty\right\}, \tag{6}$$

but only $2n+3$ equations. The determination of a unique solution requires the specification of three additional variables. With constant flight altitude and varying flight velocity, V_∞, the air density, ρ_∞, is known from the flight altitude. The relationship between speed of sound a_∞ and the true air speed V_∞ determines the Mach number M_∞. The increasing velocity can now

be tracked by the continuation process, which provides converged solutions for each eigenpair after each continued step. The total derivative of the equation system in Eq.(5) with respect to the variable parameter flight speed provides the tangent vector $\{v_i\} = \frac{d\{x\}}{dV_\infty}$:

$$\left[\frac{\partial\{y\}}{\partial\{x\}}\right]\left\{\frac{d\{x\}}{dV_\infty}\right\} - \left\{\frac{\partial\{y\}}{\partial V_\infty}\right\} = \{0\}. \tag{7}$$

It can be found by transformation of the complex equations to an equivalent real system written as Jacobian coefficient matrix multiplied by the tangent vector:

$$\begin{bmatrix} \mathrm{Re}([F]) & -\mathrm{Im}([F]) & \mathrm{Re}\left(\frac{\partial[F]}{\partial s}\{q\}\right) & -\mathrm{Im}\left(\frac{\partial[F]}{\partial s}\{q\}\right) & \mathrm{Re}\left(\frac{\partial[F]}{\partial k}\{q\}\right) \\ \mathrm{Im}([F]) & \mathrm{Re}([F]) & \mathrm{Im}\left(\frac{\partial[F]}{\partial s}\{q\}\right) & \mathrm{Re}\left(\frac{\partial[F]}{\partial s}\{q\}\right) & \mathrm{Im}\left(\frac{\partial[F]}{\partial k}\{q\}\right) \\ \mathrm{Re}(\{q\})^T & -\mathrm{Im}(\{q\})^T & 0 & 0 & 0 \\ \mathrm{Im}(\{q\})^T & \mathrm{Re}(\{q\})^T & 0 & 0 & 0 \\ 0 & 0 & 0 & 1 & -\frac{V_\infty}{c} \end{bmatrix} \begin{Bmatrix} \frac{d(\mathrm{Re}(\{q\}))}{dV_\infty} \\ \frac{d(\mathrm{Im}(\{q\}))}{dV_\infty} \\ \frac{d\sigma}{dV_\infty} \\ \frac{d\omega}{dV_\infty} \\ \frac{dk}{dV_\infty} \end{Bmatrix} - \ldots$$

$$\begin{Bmatrix} \frac{\partial(\mathrm{Re}([F]))}{\partial V_\infty}\mathrm{Re}(\{q\}) - \frac{\partial(\mathrm{Im}([F]))}{\partial V_\infty}\mathrm{Im}(\{q\}) \\ \frac{\partial(\mathrm{Im}([F]))}{\partial V_\infty}\mathrm{Re}(\{q\}) + \frac{\partial(\mathrm{Re}([F]))}{\partial V_\infty}\mathrm{Im}(\{q\}) \\ 0 \\ 0 \\ 0 \end{Bmatrix} = \{0\} \tag{8}$$

The MATLAB Toolbox MATCONT from Dhooge et al. [8] provides a numerical environment for the continuation method. The flutter equations are assumed as constant functions $f : \mathbb{R}^{n+1} \to \mathbb{R}^n$, for which the solution curve $f(\{x\}) = \{0\}$ should be calculated. For tracking purposes, it is necessary to have a starting solution $\{x_i\}$ and in addition the normalized tangent $\{v_i\}$. The calculation of the next point along the solution branch $\{x\}_{i+1}$ is composed of the following two steps: the prediction of the next point followed by the correction of that predicted point. The tangent extrapolates a new solution in direction of the continued parameter with an increment step size $h > 0$:

$$\{x^0\} = \{x_i\} + h\{v_i\}. \tag{9}$$

When the increment size h is selected small enough, the approximated solution $\{x^0\}$ is located close to the actual solution curve (see Figure 1). In order to find the next point $\{x_{i+1}\}$ on the solution branch, the Newton algorithm is applied. Therefore, a further scalar auxiliary condition must be introduced. The hyperplane at the extrapolation $\{x^0\}$ must lie orthogonally to the tangential vector $\{v_i\}$:

$$\begin{Bmatrix} \{y(\{x\})\} \\ (\{x\}-\{x^0\})^T \{v_i\} \end{Bmatrix} = \{0\}. \tag{10}$$

Newton's iteration converges based on $\{x^0\}$ to a point $\{x_{i+1}\}$ on the solution curve when the increment size h is small enough and the rank of the Jacobian matrix $\left[\frac{\partial\{y\{x\}\}}{\partial\{x\}}\right]$ is equal to n.

The derivative in the direction of the continued parameter can be calculated using finite difference procedures for every continuation step, whereby the system of equations must be solved twice. Analytical calculated sensitivities may reduce computational costs. The global sensitivity of the flutter equations in Eq.(5) with respect to flight velocity is determined by solving Eq. (8)

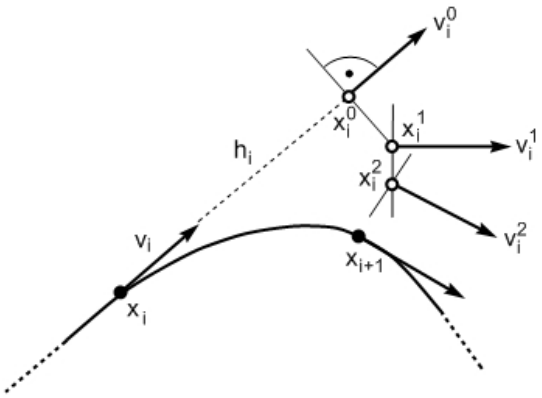

Figure 1: Tracing of solution branch

This algorithm implemented in MATCONT uses an adaptive step-size control dependent on the curvature of the continued solution branch. Therefore, if the change of the resulting frequency and damping with respect to flight velocity is marginal, only very few steps are required to trace the velocity range. On the other hand, if several solutions approach each other, which may result in rapidly changing or nearly merging damping or frequency curves, the continuation algorithm needs more sub-steps for the separation of the different solution branches.

4 UNCERTAINTY PROPAGATION IN MODAL ANALYSIS

In order to make a reliable statement on the flutter proneness of an aircraft for the intended range of operation, the interval ranges of all relevant parameters must be checked. For the uncertain variation range

$$u_{0,i} - \Delta u_i \le u_i \le u_{0,i} + \Delta u_i \tag{11}$$

statistical distributions can be assumed. For the aeroelastic stability analysis of airplane structures, the knowledge of a number of low-frequency eigenmodes with eigenfrequencies and modal masses is necessary. If an FE model is available, these data can be attained using arithmetical modal analysis. The equations of motion for a freely vibrating linear discrete system are

$$[M]\{\ddot{x}(t)\} + [C]\{\dot{x}(t)\} + [K]\{x(t)\} = \{0\}, \tag{12}$$

where $[M],[C],[K] \in \mathbb{R}^{N\times N}$ are the respective inertia, damping and stiffness matrices in N discrete physical d.o.f. and $\{x(t)\} \in \mathbb{R}^N$ contains the time-dependent deflections. The structural damping is usually assumed as a modal quantity. The dynamic characteristics of the undamped system are described with the solution of the linear eigenvalue problem

$$[K][\Phi] = [M][\Phi][\Lambda]. \tag{13}$$

Here $[\Lambda] \in \mathbb{R}^{N\times N}$ and $[\Phi] \in \mathbb{R}^{N\times N}$ are the eigenvalues and eigenvectors

$$[\Lambda] = \mathrm{diag}[\lambda_1 \dots \lambda_N] = \mathrm{diag}\left[\omega_1^2 \dots \omega_N^2\right], \qquad [\Phi] = [\phi_1 \dots \phi_N]. \tag{14}$$

The eigenvectors are usually normalized to unit modal mass $[\Phi]^T[\bar{M}][\Phi] = [I]$. The nominal FE model should already render the vibration characteristics of the airplane. The mean error and the variance of the uncertainties can then be approached as a parametric deviation of the first order of the nominal system:

$$[K] = [K_0] + [\Delta K] = [K_0] + \sum_{j=1}^{n_k} \alpha_j [K_j], \qquad [M] = [M_0] + [\Delta M] = [M_0] + \sum_{j=1}^{n_m} \beta_j [M_j]. \tag{15}$$

The nominal inertia and stiffness matrices $[M_0]$ and $[K_0]$ may be the resulting mean value of a statistical distribution of the uncertain parameters.

$$\{u\}^T = \{\alpha_1 \dots \alpha_{k_n}\ \beta_1 \dots \beta_{m_n}\} \tag{16}$$

The deviations are shown as the sum of scalable macro-elements, where each can be composed of one single finite element, groups of elements or other substructures. The partial system matrices $[K_j]$ and $[M_j]$ are scaled in such a manner, that the factors α and β are defined in the limits of the interval $[-1 \dots 1]$ and may show a statistical distribution, e.g. standardised normal distribution, unified distribution etc.. The interval characteristics of the system matrices propagate through the eigenvalues and eigenvectors from Eq.(13). Even these can be expressed through mean centred nominal values with variance:

$$[\Lambda] = [\Lambda^C] \pm [\Delta\Lambda], \qquad [\Phi] = [\Phi^C] \pm [\Delta\Phi]. \tag{17}$$

Different methods can be applied to determine the deviation of the nominal value of the pairs of eigenvalues and eigenvectors. For non-probabilistic concepts, the interval modal analysis method is presented in the following.

4.1 Interval Modal Analysis Method

In interval analysis, a pair of numbers representing the maximum and minimum values, in that the variable is expected to fall, replaces the value of the deterministic variable. Interval arithmetic rules are then used to perform mathematical operations with the interval numbers, which are also valid for each element in matrix operations. The interval can be written as mean (centred) and radius (perturbation):

$$[A^I] = [\underline{A}, \bar{A}] = [A^C - \Delta A, A^C + \Delta A], \quad [A^C] = \frac{1}{2}[\bar{A} + \underline{A}], \quad [\Delta A] = \frac{1}{2}[\bar{A} - \underline{A}] \tag{18}$$

The system matrices are not considered deterministic, but every element is defined as an interval with upper and lower limit. This manner of viewing the intervals is conducted in all mathematical operations.

The deterministic procedure of the finite-element eigenvalue analysis consists of the assembly of the parameter dependent system stiffness and mass matrices [K] and [M], after which the deterministic eigenpair implicitly satisfy Eq.(13). Assuming independent interval system matrices, Deif [7] has shown that the bounds of the exact solution set are achieved for vertex matrix combination. Therefore, the solution phase introduces only conservatism through the

artificial independence of the stiffness and mass matrix. Some algorithms have been developed that efficiently calculate the exact vertex solution of the interval eigenvalue problem. An overview is given by Moens et al. in [15]. Sim et al. [16] introduced a non-iterative procedure, which states that the lower and upper bound on the *i*th eigenvalue follow directly from two deterministic eigenvalue problems:

$$\begin{aligned}
&\left([K^C]-[S_i][\Delta K][S_i]\right)\{\underline{\phi}_i\} = \underline{\lambda}_i \left([M^C]+[S_i][\Delta M][S_i]\right)\{\underline{\phi}_i\} \\
&\left([K^C]+[S_i][\Delta K][S_i]\right)\{\overline{\phi}_i\} = \overline{\lambda}_i \left([M^C]-[S_i][\Delta M][S_i]\right)\{\overline{\phi}_i\}, \\
&[S_i] = \mathrm{diag}\left(\mathrm{sgn}\left(\phi^C_{1,i}\right),\ldots,\mathrm{sgn}\left(\phi^C_{1,n}\right)\right)
\end{aligned} \tag{19}$$

where ϕ_i^C is the *i*th centred eigenvector from the deterministic analysis at the midpoints of the system matrices $[K^C]$ and $[M^C]$. This method requires all the components of the eigenvector to have the same sign over the considered domain and does not allow the occurrence of an eigenfrequency crossover in the input parameter space.

While this interval modal analysis has been applied successfully to small problems, it has not been found practical for large simulations because the results are in many cases too conservative, i.e. it predicts the greatest possible uncertainty in the output. On the other hand, the modal transformation from physical to modal d.o.f., shown in the flutter equations Eq. (1) reduces the problem size significantly. As for flutter analysis, only the lower frequency band must be considered, which includes usually up to 10^2 modal d.o.f., in spite of $10^4 - 10^7$ in physical space of an industrial FE-model. The fundamental question is the procedure to build an expanded modal basis $[T]$, that gives good predictions for all desired ranges in the modal space dependent on the uncertain parameter space of $\{u\}$. In [2] Balmes considered a few classical solutions:

- The basis of nominal modes should include more columns than needed for the chosen frequency range under consideration: $[T] = \left[\Phi_{1\ldots m}\{u_o\}\right]$.
- The enrichment of this basis by inclusion of mode shape sensitivities with respect to uncertain parameters, which are calculated by the method of Fox and Kapoor [9], can significantly extend the range of validity:
$$[T] = \left[\left[\Phi_{1\ldots m}\{u_o\}\right] \quad \frac{\partial\left[\Phi_{1\ldots m}\{u_o\}\right]}{\partial\{u\}}\right].$$
- For multi-model basis mode shapes predictions are exact for the retained values at the lower and upper bounds of the parameter space and fairly good between those points:
$$[T] = \left[\left[\Phi_{1\ldots m}\{\underline{u}\}\right] \quad \left[\Phi_{1\ldots m}\{\overline{u}\}\right]\right].$$

Hence the eigenvalue problem from Eq.(13) can be reanalyzed in the subspace:

$$\left([T]^T\left[K^C\right][T]\right)\{\psi_i^C\} = \lambda_i^C\left([T]^T\left[M^C\right][T]\right)\{\psi_i^C\} \tag{20}$$

Restitution of responses on all physical d.o.f. is then simply given by $\{\phi_j\} = [T]\{\psi_j\}$. In practice, ortho-normalization of the expanded basis must be performed before appending the enrichment. The algorithm of Balmes [3] using singular value decomposition calculates the reduced not rank-deficient basis. If this subspace transformation is introduced in Eq.(19), approximate solutions of the lower and upper bounds can be calculated independent of the

uncertain parameters $\{u\}$:

$$\begin{aligned}
&\left([T]^T[K^C][T]-[S_i][T]^T[\Delta K][T][S_i]\right)\{\underline{\psi}_i\}=\underline{\lambda}_i\left([T]^T[M^C][T]+[S_i][T]^T[\Delta M][T][S_i]\right)\{\underline{\psi}_i\}\\
&\left([T]^T[K^C][T]+[S_i][T]^T[\Delta K][T][S_i]\right)\{\overline{\psi}_i\}=\overline{\lambda}_i\left([T]^T[M^C][T]-[S_i][T]^T[\Delta M][T][S_i]\right)\{\overline{\psi}_i\}\\
&[S_i]=\mathrm{diag}\left(\mathrm{sgn}\left(\psi^C_{1,i}\right),\ldots,\mathrm{sgn}\left(\psi^C_{1,n}\right)\right)
\end{aligned}\quad (21)$$

For each mode shape under consideration, the reanalysis of frequency and shape intervals for both combinations can thus be very fast using the following relationship:

$$\omega_i^2=\left[\left(\lambda_i^C-\Delta\lambda_i\right),\left(\lambda_i^C+\Delta\lambda_i\right)\right],\qquad \{\phi_i\}=\left[[T]\left\{\psi_i^C-\Delta\psi_i\right\},[T]\left\{\psi_i^C+\Delta\psi_i\right\}\right]. \quad (22)$$

5 UNCERTAINTY PROPAGATION IN FLUTTER ANALYSIS

In the flutter equations Eq.(1), the unsteady aerodynamic forces are induced by harmonic oscillation of the aircraft structure. For the calculation, an aerodynamic theory must be applied, that provides the aerodynamic forces for specified reduced frequencies and Mach numbers. As a widely used procedure, the well-known Doublet Lattice Method, DLM [1], has proven to be reliable and has become the aeroelastic standard procedure for the subsonic compressible flight range used by the industry for many years. One of the main advantages compared with the modern CFD-methods is the independency of the aerodynamic influence coefficient matrix with respect to the structural deflection. The aerodynamic database for a fixed geometry and several reduced frequencies and Mach numbers can be calculated in advance. During the flutter analysis, the modal air loads are generated by pre- and post-multiplication of the deflections of the mode shapes. The pressure difference $\{c_p\}$ between the upper and lower side of each elementary lifting surface element can be linked to the downwash via an aerodynamic influence coefficient matrix $[AIC]$:

$$\{c_{p,i}\}=\left[AIC\left(M_\infty,k\right)\right]\left(\frac{\partial\{\phi_i\}}{\partial x}+\frac{i\omega}{V}\{\phi_i\}\right). \quad (23)$$

The downwash of every aerodynamic element is linked to the motion of the lifting surface. Here the first term corresponds to in-phase local angle of attack and the second term to out of phase component, which results from the surface velocity perpendicular to the mean flow velocity. The transformation of the spatially distributed deflection into the local system of the lifting surfaces can be conducted by interpolation. The linearized spatial transformation can be summarized in a constant matrix, $[G]$, and its spatial derivative in flow direction, $\left[\frac{\partial G}{\partial x}\right]$, that is pre-multiplied to the interval modal matrix:

$$\{w_i\}=\left(\frac{\partial[G]}{\partial x}+\frac{ik}{c}[G]\right)\{\phi_i\}. \quad (24)$$

Using the mode shape intervals of Eq. (22), the modal aerodynamic force matrix can then be split up into the deflection-dependent interval aerodynamic stiffness and the velocity-dependent interval damping matrix, that depends on the reduced frequency and Mach number:

$$\begin{aligned}\left[Q_c^C \pm \Delta Q_c\right] &= \left[\Phi^C \pm \Delta\Phi\right]^T [G]^T [S]\left[AIC(M_\infty, k)\right]([G])\left[\Phi^C \pm \Delta\Phi\right] \\ \left[Q_k^C \pm \Delta Q_k\right] &= \left[\Phi^C \pm \Delta\Phi\right]^T [G]^T [S]\left[AIC(M_\infty, k)\right]\left(\frac{\partial[G]}{\partial x}\right)\left[\Phi^C \pm \Delta\Phi\right]\end{aligned}. \quad (25)$$

Here the matrix $[S] = \mathrm{diag}[S_1, S_2, \ldots, S_m]$ includes the surface areas of the aerodynamic elements for integration of the differential pressures to aerodynamic forces.

5.1 Interval Flutter Analysis Method

For the presented uncertainty propagation methods in modal analysis, mass-normalized mode shapes are assumed caused by the ortho-normalization process. If structural damping is neglected, the flutter equation Eq.(4) can be reformulated for fixed density and velocity but with intervals resulting from modal analysis:

$$\left[F^C \pm \Delta F\right]\{q_0 + \Delta q\} = \begin{pmatrix} [I](s_0 + \Delta s)^2 - \left(\frac{1}{2}\rho_\infty V_\infty \left[Q_C^C \pm \Delta Q_C\right]\right)(s_0 + \Delta s)\ldots \\ + \left(\left[\mathrm{diag}\left(\left(\omega^C \pm \Delta\omega\right)^2\right)\right] - \frac{1}{2}\rho_\infty V_\infty^2 \left[Q_K^C \pm \Delta Q_K\right]\right) \end{pmatrix}\{q_0 + \Delta q\} = \{0\} \quad (26)$$

In accordance to Eq. (8) the total derivative of the flutter equations with respect to the uncertain interval parameter u_i can be written the unmodified Jacobian matrix multiplied by the partial derivative:

$$\begin{Bmatrix} \frac{d(\mathrm{Re}(\{q\}))}{du_i} \\ \frac{d(\mathrm{Im}(\{q\}))}{du_i} \\ \frac{d\sigma}{du_i} \\ \frac{d\omega}{du_i} \\ \frac{dk}{du_i} \end{Bmatrix} = \begin{bmatrix} \mathrm{Re}([F]) & -\mathrm{Im}([F]) & \mathrm{Re}\left(\frac{\partial[F]}{\partial s}\{q\}\right) & -\mathrm{Im}\left(\frac{\partial[F]}{\partial s}\{q\}\right) & \mathrm{Re}\left(\frac{\partial[F]}{\partial k}\{q\}\right) \\ \mathrm{Im}([F]) & \mathrm{Re}([F]) & \mathrm{Im}\left(\frac{\partial[F]}{\partial s}\{q\}\right) & \mathrm{Re}\left(\frac{\partial[F]}{\partial s}\{q\}\right) & \mathrm{Im}\left(\frac{\partial[F]}{\partial k}\{q\}\right) \\ \mathrm{Re}(\{q\})^T & -\mathrm{Im}(\{q\})^T & 0 & 0 & 0 \\ \mathrm{Im}(\{q\})^T & \mathrm{Re}(\{q\})^T & 0 & 0 & 0 \\ 0 & 0 & 0 & 1 & -\frac{V_\infty}{c} \end{bmatrix}^{-1} \times \ldots$$

$$\begin{Bmatrix} \frac{\partial(\mathrm{Re}([F]))}{\partial u_i}\mathrm{Re}(\{q\}) - \frac{\partial(\mathrm{Im}([F]))}{\partial u_i}\mathrm{Im}(\{q\}) \\ \frac{\partial(\mathrm{Im}([F]))}{\partial u_i}\mathrm{Re}(\{q\}) + \frac{\partial(\mathrm{Re}([F]))}{\partial u_i}\mathrm{Im}(\{q\}) \\ 0 \\ 0 \\ 0 \end{Bmatrix}. \quad (27)$$

The perturbed non-linear flutter equations of the upper and lower bounds are solved by applying Newton's method available from the toolbox of the continuation method. As the nominal solution $\{x_0\}$ is already known after each converged velocity continuation step, it can be used as adequate starting vector for the iterations. The solution generally converges in very few steps, so that the uncertainty bounds in frequency and damping can be calculated during the main flutter analysis process after each new velocity step of the nominal solution.

Because of the incorporated nonlinearities, the nominal solution $\{x_0\}$ is not equal to the centred solution $\{x^c\}$. The intervals of critical damping and frequency can then be extracted from lower and upper bounds:

$$\underline{\xi} \le 100 \frac{-\sigma_0}{\sqrt{\sigma_0^2 + \omega_0^2}} \le \overline{\xi}, \qquad \underline{f} \le \frac{\omega_0}{2\pi} \le \overline{f} \tag{28}$$

6 NUMERICAL EXAMPLE

The presented methods will be applied to a glider aircraft made of carbon fibre that has a high aspect ratio wing of span on 18m. The empennage is extremely slender in order to minimize the area and minimize parasite drag. A ground vibration test was conducted with this airplane in order to determine the necessary modal parameters, based on which the calculated flutter analysis was conducted. This, in turn, is the requirement for the flight test in the high-speed range up to a speed of 110 m/s EAS, which must be proven for the airworthiness certificate up to an altitude of 5000 m. A simplified finite element beam model was composed with the knowledge of the inertia and stiffness characteristics of the primary structure. It includes 2634 physical d.o.f.. The modal deformations were transferred to the aerodynamic model of the implemented DLM by using suitable interpolation methods. With the presented continuation method, every single solution branch is successively tracked up to the upper speed limit. The algorithm calculates autonomously the step size width. The damping and frequency curves are presented in Figure 2. If the solutions of frequencies are close to each other and coupling occurs, the damping progression shows strong curvature, which allows only small increments to separate the individual solution branches. If there is only a slight change with increasing speed, then large increments are chosen. At the velocity of 91 m /s, the symmetrical fuselage-bending mode at 9.07 Hz becomes unstable because of coupling with symmetrical second wing bending mode at 7.36 Hz. As can be seen from the diagram, there is no frequency crossing of both d.o.f., only a marginal approach. Although both mode shapes have bending characteristics, they have rotational participation, which can be observed from the angular directions of the nodal lines in Figure 3. The stiffness in the tail boom dominates the exciting flutter mechanism.

The uncertainties in structural dynamics are analysed with the presented interval methods and compared to the results of the Monte-Carlo-Simulation with 500 samples. Therefore, the Young's modulus of all 73 beam elements of the primary structure may randomly vary between $\pm 10\%$ compared to the nominal value. In order to limit the uncertain parameters from the very beginning, the specification of the stiffness condition in each beam element are found at either the lower or the upper bound of the intervals. Every normalized parameter therefore indicates a uniform distribution with the two conditions -1 and 1, resulting in 2^{73} possible combinations. Normally distributed random numbers are determined by the mean value μ and its standard deviation σ. The confidence intervals of the standard normal distribution are defined as 68.3% for $\mu \pm \sigma$, 95.4% for $\mu \pm 2\sigma$, and 99.7% for $\mu \pm 3\sigma$, which means that 3σ covers almost the whole interval range. Table 1 summarizes percentile deviations of the eigenfrequencies for the eight most-flutter-relevant mode shapes calculated by the presented interval methods and Monte-Carlo-simulation (see Figure 4). From the total of 2738 initial basis shapes, 591 orthogonal shapes remain after ortho-normalization in case of the sensitivity enriched basis and in case of multi-model-basis 87 from the initial of 111, in order to approximate interval characteristics of the 37 lowest mode.

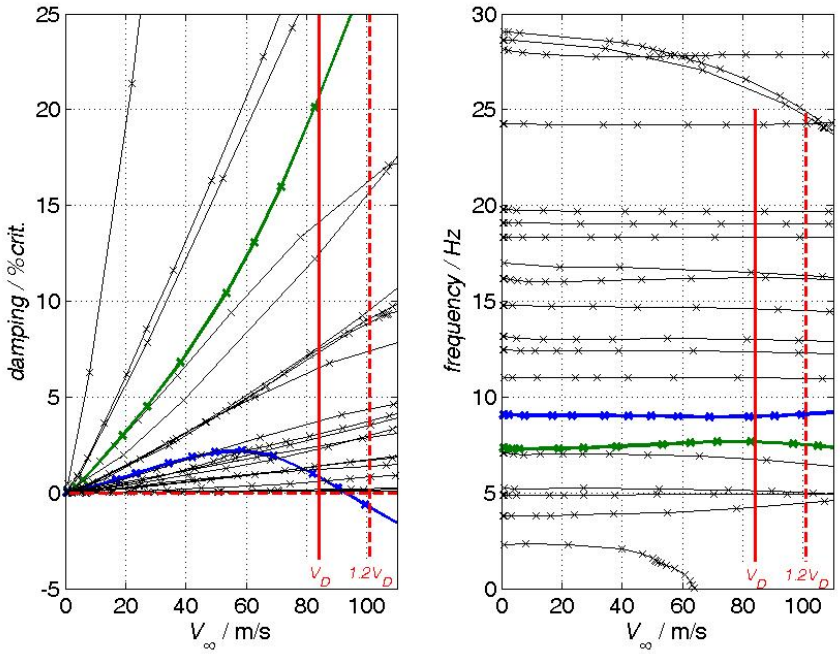

Figure 2: V-f and V-g diagrams, continuation method

Figure 3: Sym. 2nd wing bending (left), sym. fuselage bending (right)

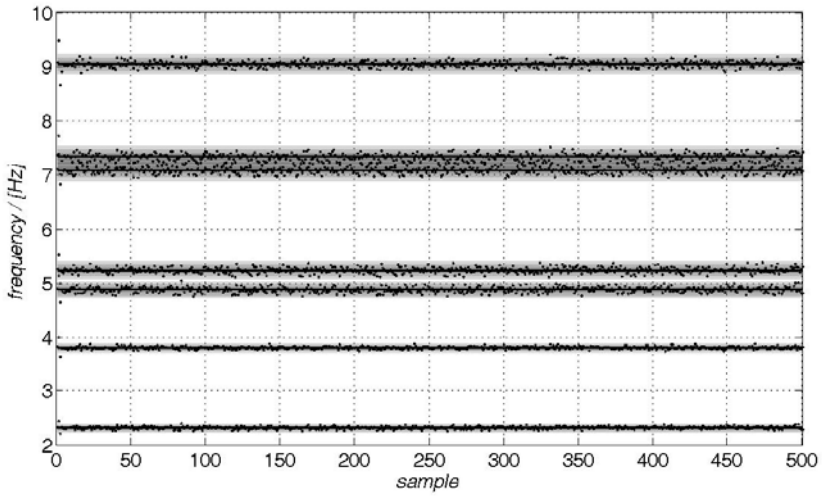

Figure 4: bounded frequencies from interval modal analysis and Monte-Carlo-method, with +/-10% stiffness uncertainty

Table 1: Comparison of frequency intervals of GVT and FEM calculated by modal basis, modal + sensitivities basis, multi model basis and Monte Carlo method (500 samples)

	FEM nominal	GVT	FEM modal basis		FEM modal + sensitivities basis		FEM multi model basis		FEM Monte-Carlo	
mode	freq. [Hz]	Δ [%]	Δ_{low}	Δ_{up} [%]	Δ_{low} [%]	Δ_{up} [%]	Δ_{low} [%]	Δ_{up} [%]	-3std [%]	+3std [%]
1st wing bend. sym.	2.34	0.00	-5.13	4.88	-4.84	5.18	-5.13	4.88	-4.03	3.15
1st fusel. bend. anti.	3.82	-10.73	-4.84	4.60	-4.83	4.61	-4.85	4.58	-2.79	1.88
1st wing bend. anti.	5.26	-4.37	-5.11	4.86	-5.11	4.86	-5.11	4.85	-3.78	2.79
1st HTP bend. anti.	7.11	-3.80	-4.05	3.80	-4.09	3.76	-4.09	3.76	-3.34	2.70
2nd wing bend. sym.	7.36	-1.49	-5.01	4.76	-5.02	4.75	-5.02	4.75	-3.24	2.31
1st fusel. bend. sym.	9.07	0.77	-4.64	4.41	-4.67	4.39	-4.67	4.38	-2.49	1.68
1st wing torsion sym.	28.15	4.09	-3.98	3.94	-4.00	3.94	-4.01	3.93	-3.00	2.31
1st wing torsion anti.	28.61	2.24	-4.23	4.04	-4.26	4.00	-4.26	4.00	-3.05	2.71

The interval bounds of eigenfrequencies from interval modal methods show good agreement with the results of the time-consuming probabilistic method. In some cases, the deterministic calculated interval ranges seem to be too conservative. The comparison with GVT results in Table 1 proves the assumption of residual uncertainties in frequencies after structural model updating, which might be non-perfect in practical. Needless to mention, there are also differences in mode shape deflections between experimental and numerical results.

For the investigation of the propagation of stiffness uncertainty in the flutter analysis the change of damping and frequencies of the two d.o.f., that are most relevant to flutter, are analyzed for increasing flight velocity using the presented continuation method. The bounds of the mode shapes and sensitivities-basis method are applied and structural damping is neglected. In Figure 5 the flutter results for all samples generated during modal Monte-Carlo-Simulation are compared with the interval flutter analysis. As the continuation method uses different intermediate steps to follow the solution branches with increasing flight velocity, the results are resampled for fixed velocity steps to statistically evaluate the mean values and standard deviations. The curves are shown with mean and confidence intervals for $\mu \pm \sigma$, $\mu \pm 2\sigma$, and $\mu \pm 3\sigma$. In comparison to the interval analysis the frequency envelopes of both d.o.f. show very good agreement for the $\mu \pm 3\sigma$ with a 99.7% confidence level. In the region of maximum damping for the unstable mode, the probabilistic results show more variance in comparison. However, the envelopes of the damping curves are significantly more conservative for the interval methods in the higher velocity range.

The histogram of the critical flutter speed in Figure 5 shows the characteristics of the normal distribution. The right and left borders of the histogram correspond to the resulting bounds of the interval analysis that shows a critical flutter speed between 85.5 m /s and 101.5 m /s. For the final interval result shown in Figure 6, all interval flutter results up to 30Hz are simultaneously calculated by continuing the nominal solution with intermediate interval perturbations using the proposed interval flutter analysis method.

7 CONCLUSIONS

The robust analysis of the flutter stability of aircraft requires a consideration of effects resulting from structural uncertainties. These uncertainties are related to production tolerances and variations in material characteristics, or to necessary simplifications of the numerical

model used for the simulation. These characteristics may be formulated in intervals with lower and upper bounds of eigenfrequencies and mode shapes, which are determined using the presented interval modal analysis. The uncertainties are tracked through the flutter analysis by applying the continuation methods for following the system response with increasing flight velocity. At every intermediate step, the perturbed flutter equations are solved for the bounds resulting from modal intervals. It is shown that the presented interval flutter analysis method calculates conservative confidence intervals of dampings and frequencies for bounded but uncertain structural parameters in critical ranges. The procedure can be extended to include uncertainties in unsteady aerodynamic forces, e.g. the aerodynamic efficiencies of control surfaces can be bounded, which otherwise can vary due to boundary layer effects. Non-linear aerodynamic effects in the transonic flight range can be introduced by bounded complex weighting factors, which are pre-multiplied to the aerodynamic influence coefficient matrix.

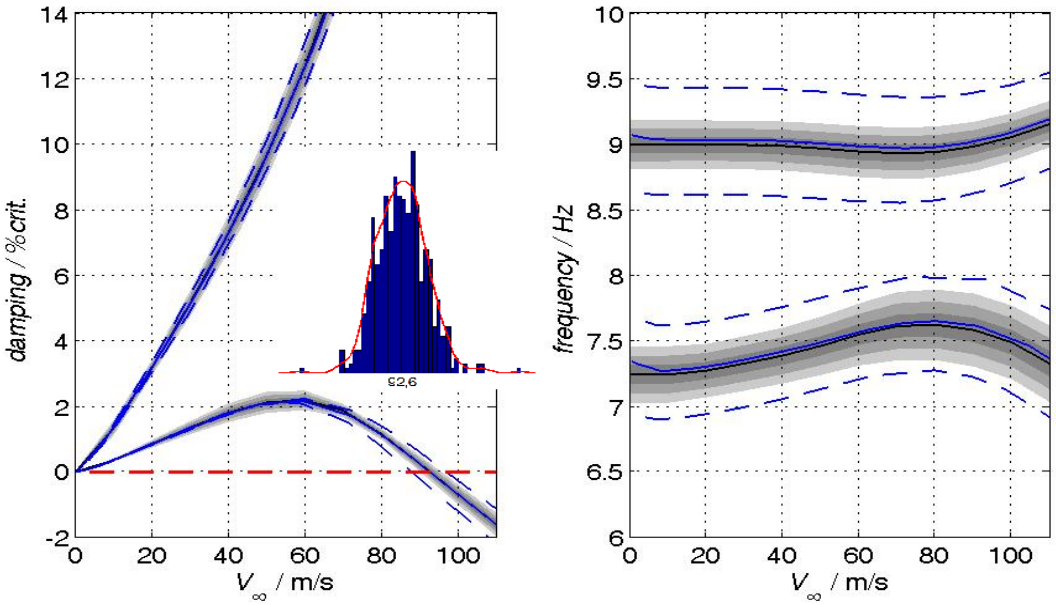

Figure 5: V-f and V-g diagrams of Monte Carlo method and interval modal analysis (--) with +/-10% stiffness uncertainty, histogram of critical flutter speeds (500 samples)

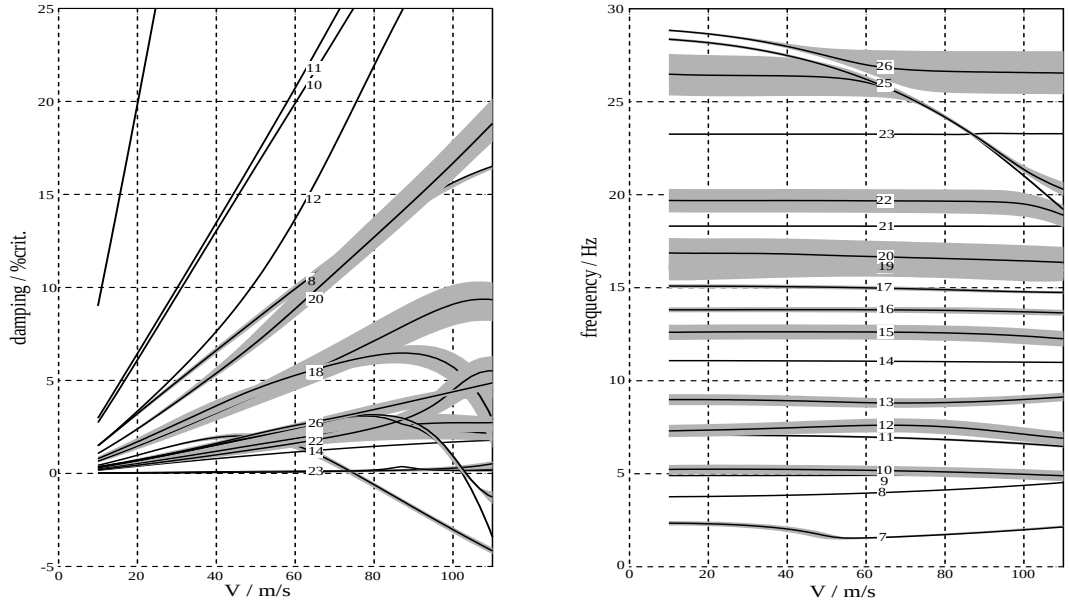

Figure 6: V-f and V-g diagrams, interval flutter method with +/-10% stiffness uncertainty

8 REFERENCES

[1] Albano, E., Rodden, W. P. (1969). A Doublet-Lattice Method for Calculating Lift Distributions on Oscillating Surfaces in Subsonic Flows. AIAA Journal, Vol. 7 No.2, pp. 279-285.

[2] Balmes, E. (1996). Parametric families of reduced finite element models. Theory and applications. Mechanical Systems and Signal Processing, Vol. 10 (1996), No. 4, pp. 381–394.

[3] Balmes, E. (1996). Optimal Ritz Vectors for Component Mode Synthesis Using the Singular Value Decomposition. AIAA Journal, Vol. 34 No. 6, pp. 1256-1260.

[4] Borglund, D. (2004). The μ-k Method for Robust Flutter Solutions. Journal of Aircraft, Vol. 41 No. 5, pp. 1209-1216.

[5] Cardani, C., Mantegazza, P. (1978). Continuation and Direct Solution of the Flutter Equation. Computers & Structures, Vol. 8 No. 3, pp. 185-192.

[6] Chen, P. C. (2000). A Damping Perturbation Method for Flutter Solution: the g-Method. AIAA Journal Vol. 38 No. 9, pp. 1519-1524.

[7] Deif, S. (1991). The interval eigenvalue problem, Zeitschrift für Angewandte Mathematik und Mechanik, No. 71, pp. 61-64.

[8] Dhooge, A., Govaerts, W., Kuznetsov, Y.A. (2003). Cl_MATCONT: A Continuation Toolbox in Matlab. Proceedings of the 2003 ACM Symposium on Applied Computing (SAC), Melbourne, FL, USA.

[9] Fox, R.L., Kapoor, M.P. (1968). Rates of Change of Eigenvalues and Eigenvectors, AIAA Journal Vol. 16 No. 12, pp. 2426–2429.

[10] Hassig, H. (1971), An Approximate True Damping Solution of the Flutter Equation by Determinant Iteration. Journal of Aircraft, Vol.8 No. 11, pp. 885-889.

[11] Lind, R., and Brenner, M. (1999). Robust Aeroservoelastic Stability Analysis, Springer–Verlag, London.

[12] Kiessling, F., Potkanski W. (1994). Nonlinear Flutter Analysis by a Continuation Method. Proc. 2nd International Conference EAHE Engineering Aero-Hydroelasticity, Pilsen, June 6-10, 1994, pp. 221-226.

[13] Kreinovich, V., Beck, J. (2007). Monte-Carlo-Type Techniques for Processing Interval Uncertainty, and Their Potential Engineering Applications. Reliable Computing, Vol. 13 No. 1, pp. 25-69.

[14] Meyer, E. E. (1988). Application of a New Continuation Method to Flutter Equations, 29th Structures, Structural Dynamics and Materials Conference, April 18-20, 1988, Williamsburg, VA, Part 3, pp.1118-1123.

[15] Moens D., Vandepitte, D. (2005). A survey of non-probabilistic uncertainty treatment in finite element analysis. Computer Methods in Applied Mechanics and Engineering, Vol. 194, Issues 12-16, pp. 1527-1555.

[16] Sim, J., Qiu, Z., Wanga, X. (2007). Modal analysis of structures with uncertain-but-bounded parameters via interval analysis. Journal of Sound and Vibration. Vol. 303, Issues 1-2, pp. 29-45.

[17] N. N.. ZAERO Version 7.3 Theoretical Manual, ZONA 02-12.4, ZONA Technology Inc., 2005.

[18] N. N.. MSC.NASTRAN Aeroelastic Analysis Users' Guide V68. MSC Software Corporation, 2004.